4-1-2012

Microstructural Characterization of Next Generation Nuclear Graphites

Chinnathambi Karthik
Boise State University

Joshua Kane
Boise State University

Darryl P. Butt
Boise State University

William E. Windes
Center for Advanced Energy Studies

Rick Ubic
Boise State University

Microsc. Microanal. 18, 272–278, 2012
doi:10.1017/S1431927611012360

Microscopy AND Microanalysis

Microstructural Characterization of Next Generation Nuclear Graphites

Chinnathambi Karthik,[1,2,*] Joshua Kane,[1,2] Darryl P. Butt,[1,2] William E. Windes,[2,3] and Rick Ubic[1,2]

[1]*Department of Materials Science and Engineering, Boise State University, 1910 University Drive, Boise, ID 83725, USA*
[2]*Center for Advanced Energy Studies, 995 University Blvd., Idaho Falls, ID 83415, USA*
[3]*Idaho National Laboratory, 2351 N. Boulevard, Idaho Falls, ID 83415, USA*

Abstract: This article reports the microstructural characteristics of various petroleum and pitch based nuclear graphites (IG-110, NBG-18, and PCEA) that are of interest to the next generation nuclear plant program. Bright-field transmission electron microscopy imaging was used to identify and understand the different features constituting the microstructure of nuclear graphite such as the filler particles, microcracks, binder phase, rosette-shaped quinoline insoluble (QI) particles, chaotic structures, and turbostratic graphite phase. The dimensions of microcracks were found to vary from a few nanometers to tens of microns. Furthermore, the microcracks were found to be filled with amorphous carbon of unknown origin. The pitch coke based graphite (NBG-18) was found to contain higher concentration of binder phase constituting QI particles as well as chaotic structures. The turbostratic graphite, present in all of the grades, was identified through their elliptical diffraction patterns. The difference in the microstructure has been analyzed in view of their processing conditions.

Key words: nuclear graphite, graphitization, transmission electron microscopy

Introduction

Nuclear graphite will be used in the next-generation very-high-temperature gas-cooled reactors owing to its excellent moderating properties (owing to its high scattering and low absorption cross section), high thermal stability, compressive strength, easy machinability, and cost-effectiveness (Allen et al., 2008). Graphite will be used as a structural as well as moderator material. Even though the earlier gas-cooled reactors (e.g., Magnox, advanced gas reactor, etc.) demonstrated the feasibility of using graphite for commercial power-producing reactor components, the historic nuclear grades of graphite no longer exist; therefore, it is imperative to characterize the new grades of graphite and demonstrate that they exhibit acceptable properties in both the nonirradiated and irradiated state. Furthermore, the microstructure-property relation in irradiated nuclear graphites is poorly understood, probably due to the complexity of the microstructure.

Single crystalline graphite has a layered structure formed by stacking of sheets of hexagonal rings of carbon atoms (graphene). The commonly found hexagonal structure of bulk graphite results from the ABAB, stacking of these graphene sheets perpendicular to the *c*-axis (Fig. 1). The distance between these sheets, also called as basal planes, is 0.335 nm. The bonding between the individual layers is relatively weak resulting in more open space between the layers and highly anisotrophic physical properties. Nuclear graphite is an artificially-produced high-purity, polycrystalline material with a complex microstructure (Nightingale, 1962). It is manufactured from coke particles (petroleum or pitch coke). Petroleum coke is obtained as a by-product of refining petroleum crude, whereas pitch coke is derived from coal tar, which is obtained as a by-product during the carbonization of coal. Coke is basically a carbonaceous material containing lamellar domains of large polycyclic aromatic molecules along with small quantities of ash and other impurities. Filler particles are manufactured by calcining the raw coke at temperatures around 1300°C to remove the volatile hydrocarbons. This calcined coke is then crushed and sized as needed. These filler particles are mixed with a pitch binder at ~165°C. Binder is a thermoplastic material, composed of thousands of different hydrocarbons (mostly aromatic compounds), derived from the distillation of coal tar. The resulting filler-binder mixture is cooled and formed into a rigid green body (via extrusion, molding, or isostatic pressing). The green body is baked at 1000°C, which results in the pyrolysis of the pitch and hence the evolution of a large volume of volatile gas. The baked material is impregnated further with pitch binder to increase the density and graphitized in an inert atmosphere at temperatures ranging from 2,500 to 3,000°C for several weeks. This process results in a polycrystalline material with a complex microstructure constituting several different graphite phases such as filler particles, binder phase, and quinoline insoluble (QI) particles (from the binder) (Nightingale, 1962; Jones et al., 2008; Wen et al., 2008*a*, 2008*b*). It also contains a large volume of macro- and micropores, resulting from gas evolution, as well as macro- and microcracks (also called Mrozowski cracks) (Wen et al., 2008*a*). Graphite has a very high *c*-axis

Received March 16, 2011; accepted September 16, 2011
*Corresponding author. E-mail: karthikchinnathambi@boisestate.edu

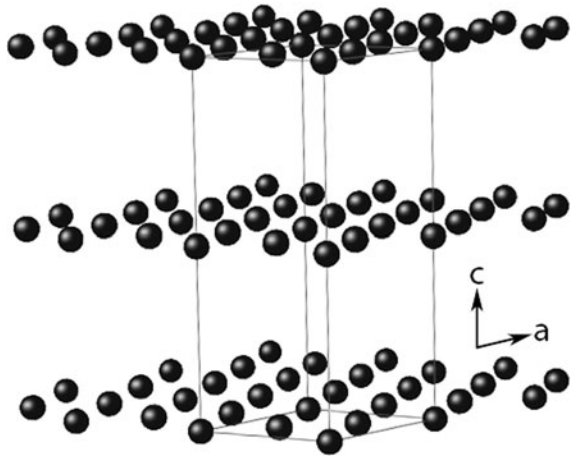

Figure 1. Schematic showing the layered crystal structure of graphite along with the unit cell outline.

thermal expansion coefficient, and a large contraction on cooling from graphitization temperatures results in the formation of microcracks. These microcracks form as a result of delamination of the graphite basal planes and hence are aligned parallel to them. The width of these microcracks varies from nano- to micrometer scale while their length is on the micrometer scale.

The fast neutron damage of graphite moderators leads to the displacement of carbon atoms that significantly modifies the microstructure and hence the bulk properties. Under irradiation, graphite crystallites undergo dimensional changes that involve expansion along the *c*-axis and shrinkage parallel to the basal planes (Nightingale, 1962; Brocklehurst & Kelly, 1993). The common explanation for these changes is that the ballistic displacement of carbon atoms caused by irradiation results in the accumulation of interstitials between the basal planes, forcing them apart (Thrower & Reynolds, 1963; Heerschap & Schüller, 1969). These interstitial carbon clusters eventually rearrange to become new basal planes, resulting in the expansion along the *c*-axis with a concurrent shrinkage along the *a*-axis postulated to be due to the collapse of basal-plane vacancies. In polycrystalline graphite, the microcracks can accommodate the *c*-axis expansion resulting in net shrinkage at lower doses of irradiation (Bollmann, 1961).

Ballistic displacement of atoms also results in significant creep even at room temperature (Simmons, 1965), whereas significant thermal creep requires very high temperatures in excess of 2000°C. The irradiation induced point defects result in an increased Young's modulus (attributed to the pinning of dislocations) and a decrease in thermal conductivity (due to increased phonon scattering by vacancy clusters) (Wu et al., 1994). Since all of these processes alter the microstructure, it is important to fully understand the virgin microstructure-property relationship of each new grade. In this article, the authors have investigated and compared the microstructural features of three different commercial grades of nuclear graphite, NBG-18 and PCEA, which are new grades with potential applications in the next generation reactors, as well as IG-110, which is a historic reference grade.

Materials and Methods

Transmission electron microscope (TEM) samples of these graphites were prepared by conventional sample preparation techniques. Bulk samples of NBG-18 (SGL Group, Wiesbaden, Germany), PCEA (GrafTech International, Parma, OH, USA), and IG-110 (Toyo Tanso Co., Kagawa, Japan) were obtained from the manufacturers. Disks of 3 mm diameters were cut from the as-received bulk graphite using a diamond saw. These disks were further thinned mechanically to approximately 20–30 μm thick. A precision ion polishing system (Gatan PIPS 691; Gatan, Inc., Pleasanton, CA, USA) was used to achieve the final electron transparency. Ion-milling conditions were optimized to minimize the ion-beam damage. Typically, the samples were milled for about 60–70 min at 5° followed by a low angle milling step at 2° for 10 min. Electron microscopy studies were performed at room temperature on a 200 kV JEOL-2100 high-resolution TEM (JEOL Ltd., Tokyo, Japan).

Results and Discussion

Figure 2 shows the various microstructural features of the IG-110, which is fine-grained isotropic graphite fabricated via cold isostatic pressing. Petroleum coke is used as the filler material. Figure 2a shows what appears to be a filler particle (marked F) surrounded by binder (marked B) on both sides. The filler particles are lenticular in shape with sizes varying from a few tens of nanometer to tens of micrometers in length. The width varies from a few tens of nanometers to hundreds of nanometers. The lenticular shape arises from the shape of the starting coke particles. When the highly crystalline coke particles are crushed, they cleave parallel to basal planes resulting in a powder containing elongated particles with their crystallographic *c*-axes perpendicular to the length of the particles (Nightingale, 1962). This means that the shape of the resultant filler particles depends on the crystallinity of the coke used. Petroleum coke is usually highly crystalline whereas pitch coke is usually less crystalline, resulting in more spherical filler particles. It should also be noted that the quality of the coke can vary depending on the crude oil/coal-tar pitch source used, affecting the shape distribution of the resultant filler particles significantly. Figures 2b and 2c are at a higher magnification and show the filler particles in different regions. The filler particles (as well as the binder) contain cracks running parallel to the basal planes. Microcracks are believed to form through delamination of the basal planes as a result of thermal contraction and play a major role in the irradiation induced swelling process as well as the thermal expansion characteristics of the graphite. It was originally thought that these cracks would be void of any material; but interestingly, most are filled with amorphous carbon, the origin of which is not clear. This observation is in accordance with the recent study by Wen

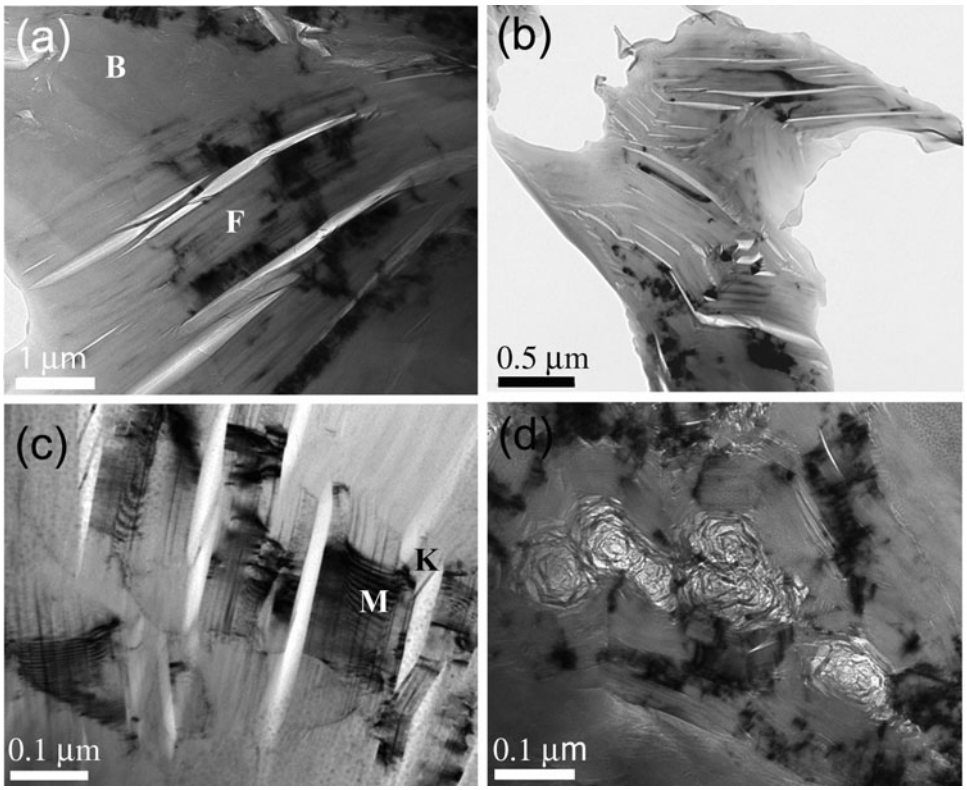

Figure 2. Bright-field TEM micrographs of IG-110 grade graphite: (**a**) interface region between a filler particle (marked F) and binder (marked B), (**b**) filler particle at high magnification, (**c**) filler particle with kink boundaries (marked K) and moiré fringes (marked M), and (**d**) binder region.

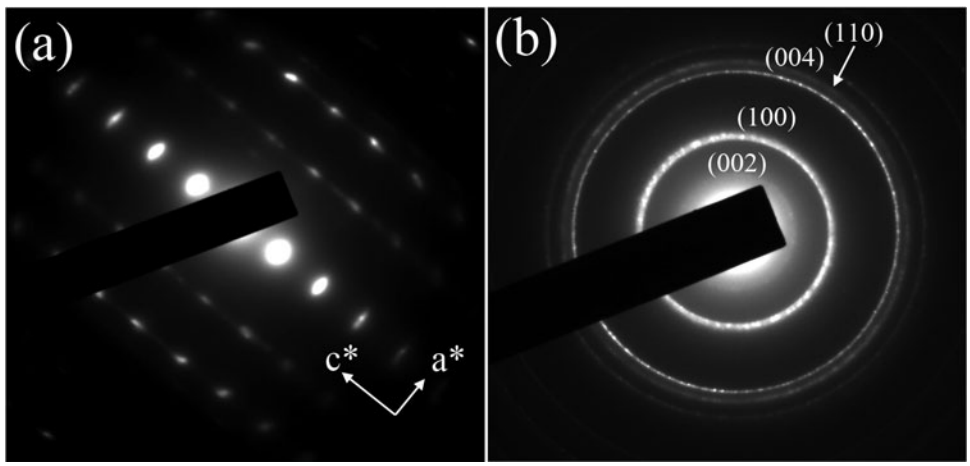

Figure 3. SAED diffraction patterns recorded from (**a**) filler particle and (**b**) rosette in the binder region of IG-110 graphite.

et al. (2008*a*), who, despite preparing samples using several methods, noticed the presence of amorphous carbon in the microcracks in PGA grade nuclear graphite. The present authors show that this is a characteristic of all nuclear graphites irrespective of the manufacturing process and is found to be present in all the graphite grades under study.

Figure 2c shows the presence of delamination cracks with strands of inclined basal planes (marked K) bridging the bulk of the crystal across the cracks. These inclined strands, commonly known as kink bands, arise as a localized deformation mechanism in a variety of materials. Materials with layered structure such as graphite, boron nitrides, etc., subjected to compressive stresses, are especially prone to this kind of localized deformation (Barsoum et al., 2004). Another interesting feature of Figure 2c is the presence of moiré fringes (marked M), which indicates the presence of twist boundaries that is confirmed by the selected area electron diffraction (SAED) pattern shown in Figure 3a. The [010] pattern clearly shows the arcing of the spots, indicat-

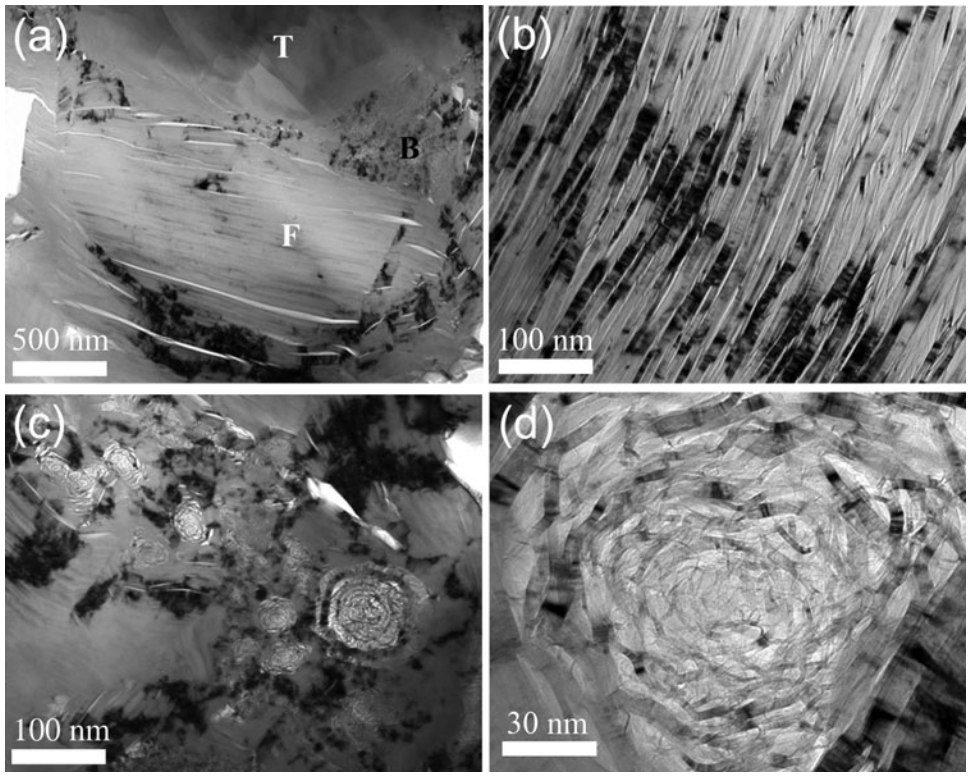

Figure 4. Bright-field TEM micrographs of NBG-18 grade graphite: (**a**) interface region constituting filler (marked F), binder (marked B), and turbostratic graphite (marked T), (**b**) filler particle at higher magnification, (**c**) binder region, and (**d**) rosette (QI particle) at high magnification.

ing the presence of low-angle twist boundaries that may be a result of the delamination process.

Figure 2d shows a micrograph recorded from the binder region. The binder region was found to contain well-graphitized crystallites of carbon with occasional rosette-structured particles embedded in them. Binder regions were also found to contain cracks similar to that of the filler particles. The rosette-shaped particles are well crystallized and are thought to originate from the QI fraction present in the pitch (Nightingale, 1962). Even though it is very difficult to quantify the concentration of these particles using TEM due to the limited field of view and heterogeneity of microstructure, the authors estimated about 10–20 particles per square micron in the binder region. The size of these rosettes varied from 10 nm to a few hundreds of nanometers in diameter. The SAED pattern recorded from a rosette is shown in Figure 3b with the prominent rings indexed as (002), (100), (004), and (110) planes. The ring pattern is a result of the continuous spiraling of the graphitic strands, which is equivalent to texturing in a direction perpendicular to the *c*-axis.

QI particles are basically solid particles similar to carbon black, composed of high-molecular-weight hydrocarbons (Mochida et al., 1978; Peaden et al., 1980). These are formed either during the decomposition of coal or through the condensation of small aromatic molecules on the walls of the cracking chamber. It is believed that the aromatic molecules result in rosette-shaped particles constituting a spiral of graphite strands during graphitization. These strands are more disordered at the center of the rosettes. It can also be seen that these rosettes act as templates inducing the graphitization of binder around them in the form of wide concentric strands of graphite (marked with a dotted arrow in Fig. 2d) retaining the crystallographic orientation of the outermost strand of the rosette. The concentration of QI particles in coal tars can vary from 2 to 12 wt% depending on the type of coal used and the production conditions. Unfortunately, the exact concentrations are proprietary and so not revealed by the manufacturers.

The presence of QI particles has been known to affect the mechanical properties of graphite (Morgan et al., 1960). Studies have shown the compressive strength of graphite to vary significantly with QI particle concentration, and there appears to be an optimum concentration where compressive strength is maximized. During baking, QI particles provide paths facilitating the escape of volatile species that reduces cracking and hence increases the strength of the final product (Morgan et al., 1960).

Figure 4 shows the microstructural features of NBG-18 grade graphite. NBG-18 is vibrationally molded, near-isotropic graphite with pitch coke as the filler source. Figure 4a shows an interface region between a filler particle (marked F), binder phase (marked B), and turbostratic graphite (marked T). Figure 4b shows the close-up view of a filler particle delaminated into several fine stands (~10 nm in width) of graphite resulting in numerous microcracks.

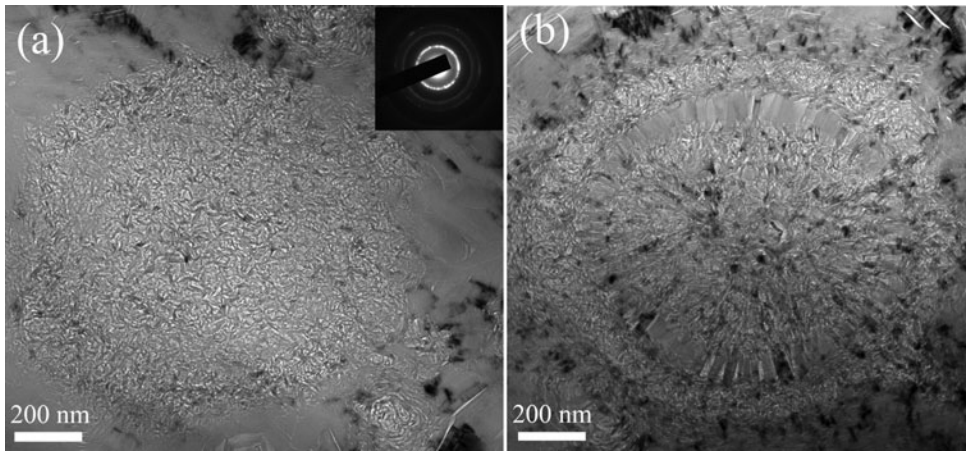

Figure 5. Bright-field TEM micrographs of spherical chaotic structures in NBG-18 grade graphite. Inset in (**a**) shows a typical SAED pattern recorded from these structures.

Several filler particles with such fine strands were observed while other particles exhibited only a few cracks, similar to IG-110. One of the striking features of the NBG-18 microstructure is the high concentration of binder and QI particles (Fig. 4c) compared to other grades under study. The authors observed the presence of 40–60 QI particles of varying sizes in a given square micron of binder. One of the reasons for the high concentration of the QI particles could be the usage of coal-tar pitch (as the binder source), which naturally tends to have a high concentration of QI particles (Nightingale, 1962). Figure 4d is a high-magnification image depicting the internal structure of a QI particle, and the diffraction pattern obtained was similar to that in Figure 3b. The interior of QI particles appears to be more chaotic in case of NBG-18 compared to other grades.

Apart from the QI particles, the binder phase in NBG-18 showed the presence of several other types of spherical chaotic structures as shown in Figure 5. These structures are of $\sim$1 μm in diameter and packed with randomly oriented well-crystallized graphitic strands. Similar structures have been observed in PGA grade graphite (Wen et al., 2008*b*), which has a coal-tar pitch binder; therefore, it can be safely concluded that these structures are characteristic of coal-tar pitch based binders. The diffraction patterns recorded from these chaotic structures were similar to those of QI particles.

The microstructural features of PCEA graphite, which is a nearly-isotropic, extruded, petroleum coke based graphite, are depicted in Figure 6. Figure 6a shows an interface region between a filler particle (marked F) and binder phase (marked B) with embedded QI particles. Figure 6b shows the structure of a filler particle with microcracks. The microcracks in the case of PCEA appear to be wider than in other grades. Another distinct feature of PCEA is that the amorphous carbon filling the microcracks contains numerous voids. The sizes of these voids were found to vary in the range of approximately 1–25 μm in diameter. Figures 6c and 6d show the microstructure of the binder phase and a QI particle, respectively. The concentration of QI particles is comparable to that of IG-110. It should be noted that, unlike NBG-18, petroleum based pitch is used in the production of both IG-110 and PCEA, so they are expected to have negligible amounts of QI particles.

Apart from the above-mentioned structures that constitute well-crystallized graphite, the authors also noticed the presence of turbostratic graphite in all the graphite grades. Figure 7 shows a typical microstructure of turbostratic graphite and the corresponding SAED pattern recorded from IG-110. Turbostratic graphites can be identified in a TEM by their elliptical diffraction patterns. Turbostratic graphite has close-packed carbon planes that are curled and rotated with respect to each other. In turbostratic graphite, the atoms are arranged in layers similar to graphite, but stacked randomly. The presence of simultaneous translational and rotational disorder results in the distribution of the scattering power in the reciprocal lattice in the form of concentric cylinders. The sectioning of these cylinders by the Ewalds sphere gives rise to a series of elongated spots that lie on one ellipse (Schiffmacher et al., 1980). As pointed out by Vainshtein et al. (1992), one could index the spots on one ellipse with the same hk indices but with different l indices as shown in Figure 7b. Turbostratic graphite can form during the process of graphitization or normal graphite can be converted to the turbostratic form by weakening the bonding between the layers by, for example, mechanochemical activation (Salver-Disma et al., 1999). There is also a possibility of the accidental insertion of Ar^+ ions between the layers during ion-milling resulting in turbostratic graphite. To verify this, TEM studies were carried out on powdered samples of graphite by dispersing the flakes of graphite particles on a TEM grid. TEM studies (Fig. 8) showed the turbostratic graphite to be present even in the case of the powder samples. It confirms that the turbostratic graphite is an inherent characteristic of the nuclear graphite microstructure and not an artifact created by ion-milling.

There have been several attempts in recent times to model the irradiation-induced property changes in graphite, especially Young's modulus and dimensional changes,

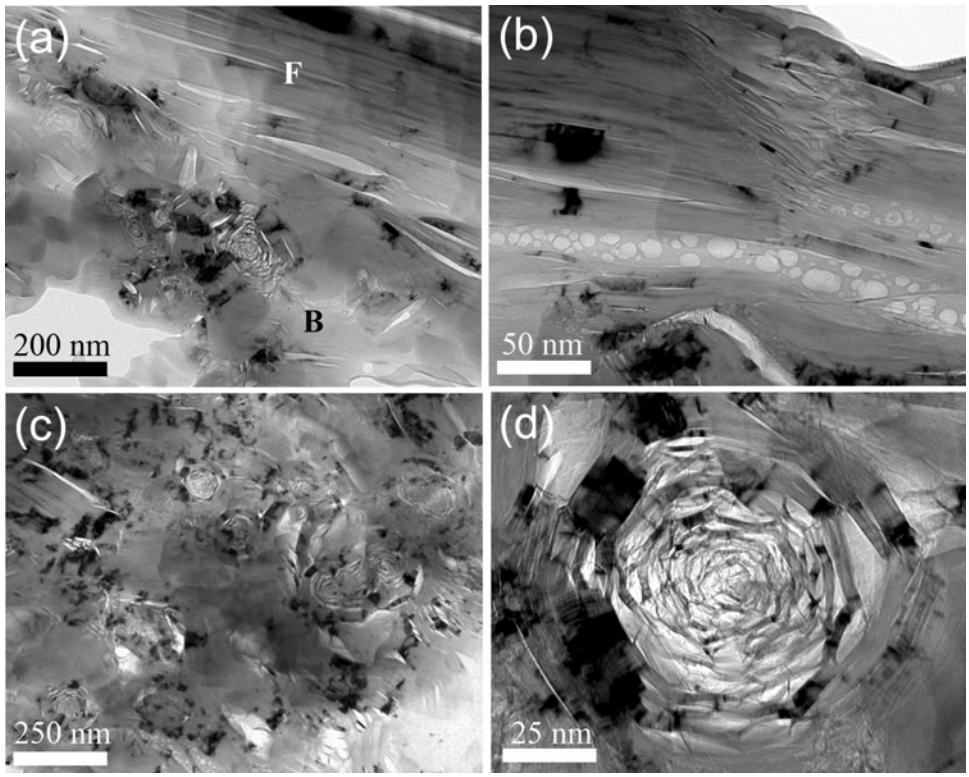

Figure 6. Bright-field TEM micrographs of PCEA grade graphite: (**a**) interface region constituting filler (marked F) and binder phase (marked B), (**b**) filler particle with cracks filled with porous amorphous carbon, (**c**) binder region, and (**d**) a rosette at high magnification.

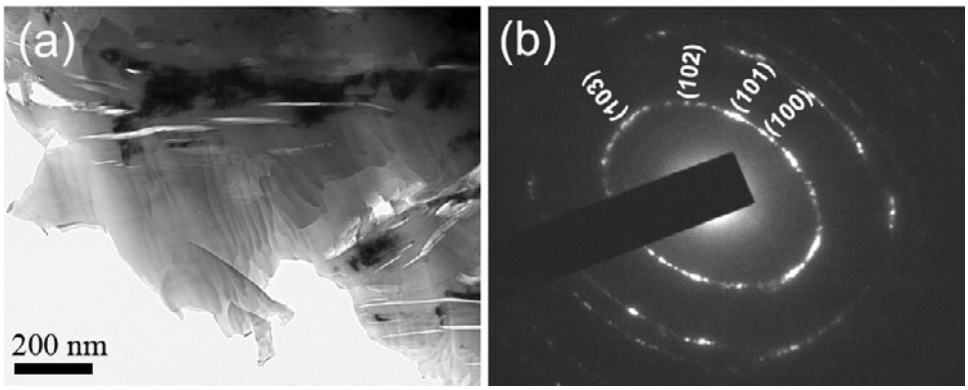

Figure 7. (**a**) Bright-field TEM micrograph of turbostratic graphite recorded from IG-110 grade graphite and (**b**) the corresponding SAED pattern.

and to identify the probable microstructural mechanisms (Hall et al., 2006; Bradford & Steer, 2008). These studies show that the changes in the physical properties under irradiation are highly dependent on the filler particle size as well as the porosity; however, the experimental results obtained from various test reactors have shown these changes to be highly complex providing very little insight into the microstructural mechanisms (Simmons, 1965). One of the reasons for the difficulty is the poor understanding of the part microstructure plays in defining the properties, and the authors hope that this article adds valuable information on that front.

Conclusions

The microstructure of various grades of next generation nuclear graphite has been studied by using transmission electron microscopy. Bright-field imaging was carried out to characterize the different constituents such as filler, binder, and microcracks that constitute the complex microstructure of the nuclear graphite. The size and shape of the microcracks were found to be different for different grades. The pitch based graphite contains higher concentration of binder phase as well as QI particles compared to other grades, which is attributed to the source of the binder (coal-tar

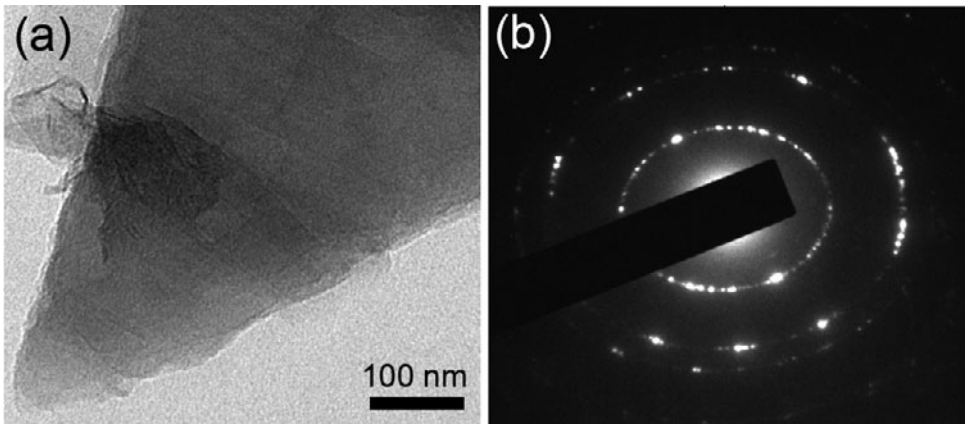

Figure 8. (**a**) Bright-field TEM micrograph and (**b**) SAED diffraction recorded from powdered sample of IG-110 showing the presence of turbostratic carbon.

pitch). The presence of turbostratic graphite in all of the grades under study was also observed.

Acknowledgments

This material is based upon work supported by the Department of Energy (National Nuclear Security Administration) under Award Numbers 00041394/00026 and DE-NE0000140. TEM studies were carried out at the Boise State Center for Materials Characterization (BSCMC) and were supported by National Science Foundation MRI grant DMR-0521315. Furthermore, J.K. acknowledges the funding of the Nuclear Regulatory Commission under the Nuclear Materials Fellowship Program (NRC-38-08-955).

References

Allen, T.R., Sridharan, K., Tan, L., Windes, W.E., Cole, J.I., Crawford, D.C. & Was, G.S. (2008). Materials challenges for Generation IV nuclear energy systems. *Nucl Technol* **162**, 342–357.

Barsoum, M.W., Murugaiah, A., Kalidindi, S.R., Zhen, T. & Gogotsi, Y. (2004). Kink bands, nonlinear elasticity and nanoindentations in graphite. *Carbon* **42**, 1435–1445.

Bollmann, W. (1961). Electron microscope study of radiation damage in graphite. *J Appl Phys* **32**, 869–877.

Bradford, M.R. & Steer, A.G. (2008). A structurally-based model of irradiated graphite properties. *J Nucl Mater* **381**, 137–144.

Brocklehurst, J.E. & Kelly, B.T. (1993). The dimensional changes of highly-oriented pyrolytic graphite irradiated with fast neutrons at 430°C and 600°C. *Carbon* **31**, 179–183.

Hall, G., Marsden, B.J. & Fok, S.L. (2006). The microstructural modelling of nuclear grade graphite. *J Nucl Mater* **353**, 12–18.

Heerschap, M. & Schüller, E. (1969). Vacancy and interstitial loops in graphite single crystals reactor-irradiated at 900° and 1200°C. *Carbon* **7**, 624–625.

Jones, A.N., Hall, G.N., Joyce, M., Hodgkins, A., Wen, K., Marrow, T.J. & Marsden, B.J. (2008). Microstructural characterisation of nuclear grade graphite. *J Nucl Mater* **381**, 152–157.

Mochida, I., Maeda, K. & Takeshita, K. (1978). Comparative study of the chemical structure of the disk-like components in the quinoline insolubles. *Carbon* **16**, 459–467.

Morgan, M.S., Schlag, W.H. & Wilt, M.H. (1960). Surface properties of the quinoline-insoluble fraction of coal-tar pitch. *J Chem Eng Data* **5**, 81–84.

Nightingale, R.E. (1962). *Nuclear Graphite*. New York: Academic Press.

Peaden, P.A., Lee, M.L., Hirata, Y. & Novotny, M. (1980). High-performance liquid chromatographic separation of high-molecular-weight polycyclic aromatic compounds in carbon black. *Anal Chem* **52**, 2268–2271.

Salver-Disma, F., Tarascon, J.M., Clinard, C. & Rouzaud, J.N. (1999). Transmission electron microscopy studies on carbon materials prepared by mechanical milling. *Carbon* **37**, 1941–1959.

Schiffmacher, G., Dexpert, H., Caro, P. & Cowley, J.M. (1980). Elliptic electron diffraction pattersn from the films of turbostratic graphite. *J Microsc Spectrosc Electron* **5**, 729–734.

Simmons, J.W.H. (1965). *Irradiation Damage in Graphite*. New York: Pergamon Press.

Thrower, P.A. & Reynolds, W.N. (1963). Microstructural changes in neutron-irradiated graphite. *J Nucl Mater* **6**, 221–226.

Vainshtein, B.K., Zuyagin, B.B. & Avilov, A.V. (1992). Electron diffraction structure analysis. In *Electron Diffraction Techniques I*, Cowley, J.M. (Eds.). New York: Oxford University Press.

Wen, K.Y., Marrow, J. & Marsden, B. (2008*a*). Microcracks in nuclear graphite and highly oriented pyrolytic graphite (HOPG). *J Nucl Mater* **381**, 199–203.

Wen, K.Y., Marrow, T.J. & Marsden, B.J. (2008*b*). The microstructure of nuclear graphite binders. *Carbon* **46**, 62–71.

Wu, C.H., Bonal, J.P. & Thiele, B. (1994). Thermal conductivity changes in graphites and carbon/carbon fiber materials induced by low neutron damages. *J Nucl Mater* **212–215**, 1168–1173.